Bistability driven by white shot noise

J. M. Porrà and J. Masoliver
Departament de Física Fonamental, Universitat de Barcelona, Diagonal, 647, 08028-Barcelona, Spain
(Received 10 September 1992)

We consider mean-first-passage times and transition rates in bistable systems driven by white shot noise. We obtain closed analytical expressions, asymptotic approximations, and numerical simulations in two cases of interest: (i) jumps sizes exponentially distributed and (ii) jumps of the same size.
PACS number(s): 05.40+j, 05.60+w, 05.20Dd, 05.90+m

I. INTRODUCTION

In recent years much attention has been devoted to the study of mean-first-passage times (MFPT's) and transition rates of bistable systems driven by colored noise [1–4]. In such systems the noise can induce transitions between the two stable states and the magnitude that usually characterizes the transitions is the transition rate, i.e., the frequency at which the transition takes place. Under fairly general conditions the transition rate is related to the mean-first-passage time from one stable state to the other.

There are several techniques available to calculate MFPT's depending on the nature of the noise. Among these the *stochastic trajectory analysis technique* (STAT) is particularly useful when the driving noise can only take on a small number of values, as is the case of dichotomous noise and shot noise. In two recent papers [3, 4] we have considered bistable systems driven by dichotomous noise and our aim in this paper is to study bistable systems driven by white shot noise (WSN). Thus we will consider one-dimensional processes whose dynamical evolution equation is of the form

$$\dot{X}(t) = f(X) + F(t) \ , \tag{1}$$

where $f(x) = -V'(x)$ and $V(x)$ is a bistable potential. $F(t)$ is the random driving process

$$F(t) = \sum_i \gamma_i \delta(t - \tau_i) - a \ , \tag{2}$$

where a is a parameter to be adjusted in order to have a zero-centered noise, i.e., $\langle F(t) \rangle = 0$ and $\{(\tau_i, \gamma_i),\ i = 1, 2, 3, ...\}$ is a sequence of random points in the plane (τ, γ) with $\{\gamma_i\}$ independent of $\{\tau_i\}$. Therefore, the random process $F(t)$ may be viewed as a sequence of pulses at random times τ_i, each pulse having an independent random weight γ_i. The effect of this input noise on the output of the system (1) is a series of independent random jumps in the trajectory—that is, a discontinuous trajectory with the discontinuities of independent random heights occurring at random times.

We will assume that $\{\tau_i\}$ is a sequence of Poisson points. In this case the time intervals $t_i = \tau_i - \tau_{i-1}$ constitute a renewal process with the exponential "switch distribution"

$$\psi(t) = \lambda e^{-\lambda t} \ . \tag{3}$$

We will also assume that the random variables $\{\gamma_i\}$ are positive and uncorrelated with a given probability density function $\chi(\gamma_i)$. We will consider two particular "jump distributions." The exponential distribution is given by

$$\chi(\gamma_i) = \frac{1}{\gamma} e^{-\gamma_i/\gamma} \quad (\gamma_i \geq 0), \tag{4}$$

where $\gamma > 0$ is the mean size of the jumps, and the delta-function distribution

$$\chi(\gamma_i) = \delta(\gamma_i - \gamma) \ , \tag{5}$$

i.e., all jumps are of the same size $\gamma > 0$.

For both jump distributions, the condition that $F(t)$ is zero centered implies that

$$a = \lambda\gamma. \tag{6}$$

One can easily see from Eqs. (1)–(5) that the input noise is WSN, that is, the shot noise is δ correlated

$$\langle F(t)F(t') \rangle = 2D\delta(t - t') \ , \tag{7}$$

where

$$D = \gamma^2\lambda = \frac{a^2}{\lambda} \tag{8}$$

for exponential distributed jumps and

$$D = \frac{\gamma^2\lambda}{2} = \frac{a^2}{2\lambda} \tag{9}$$

for jumps of the same size. We also note that WSN is characterized for having all its cumulants δ correlated in time [5]. Moreover, WSN with exponentially distributed jumps, Markovian dichotomous noise, and Gaussian white noise are related to each other by means of suitable limits [6, 7].

In what follows we will assume that the potential $V(x)$ has two minima at x_1 and x_2 and one maximum at x_u. Thus, in the absence of noise the time evolution of the system is towards one of the potential wells. The existence of two stable states x_1 and x_2 and one unstable state x_u divides the coordinate space in two regions A and B. If the initial position $x_0 < x_u$ (i.e., the system is

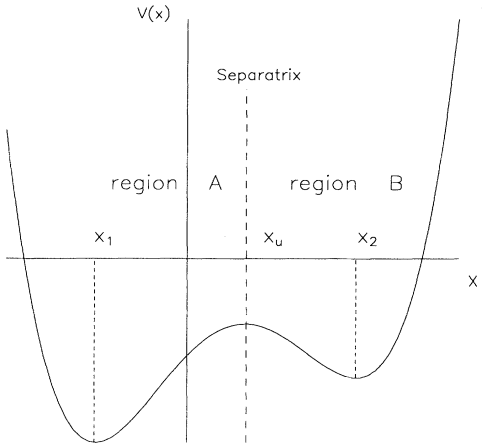

FIG. 1. Bistable potential function. The separatrix, at $x = x_u$, divides the coordinate space in two regions: A and B.

initially in region A), then $X(t)$ will evolve towards x_1, while if $x_0 > x_u$ (i.e., x_0 in region B), the system will evolve towards x_2. A and B are the *basins of attraction* and x_u is the *separatrix* (see Fig. 1).

In the presence of noise the system can jump from one basin of attraction to the other and the system can experience a *noise-induced transition*. In order to properly define transition rates for this case one must assume that (i) the system stays for a long time in a neighborhood of one of the stable points and (ii) transitions are suddenly occurring in times very short compared with the time of residence in regions A or B. The separation of time scales implies that the parameter D is small. We note that the assumption of small D is also needed for any kind of input noise [1]. Moreover, for a transition to exist in both directions, i.e., from x_1 to x_2 or vice versa, the parameter a must be larger than some critical value a_c. This last assumption has been used also in bistable systems driven by dichotomous noise [3]. We finally observe that the process is bounded on the left by the value x_s defined by

$$f(x_s) - a = 0. \tag{10}$$

We refer the reader to the Appendix for details.

This paper is organized as follows. The expressions for the MFPT in the cases of interest are found in Sec. II. For shot noise with jumps exponentially distributed, transitions rates are calculated in Sec. III, while in Sec. IV we discuss the MFPT to reach the top of the potential barrier. In Sec. V, some calculations for shot noise with jumps of the same size are shown, and conclusions are drawn in Sec. VI. Finally, in the Appendix we study the *phase diagram* of the system.

II. MEAN-FIRST-PASSAGE TIMES

In bistability problems one is interested in the MFPT to a single critical level, such as a stable or an unstable state. Using STAT, Masoliver [8] obtained closed analytical expressions of the MFPT to one critical level, say z, for processes driven by noncentered shot noise. In [8] the MFPT depends on two constants that are found by means of two *exact* boundary conditions: One involving the critical level z and taking into account the absorbing nature of z and the other one involving the *natural barrier* x_s of the process [cf. Eq. (10)]. In previous works, Van den Broeck and Hänggi [9] obtained the same differential equation for the MFPT as that of Masoliver, but with different boundary conditions which do not take into account the absorbing nature of the level z. Also Hänggi and Talkner [10] and Hernández-Garcia *et al.* [11] used the correct boundary condition, but only studied the free case, i.e., $f(x) = 0$. On this point we mention that the obtention of correct boundary conditions for non-Markovian processes is a difficult task which only recently has been correctly addressed for some cases [8, 10, 12]. In this section we will apply the results of [8] to calculate MFPT for centered shot noise.

In order to apply the results of [8] to the centered noise (2) we have to turn Eq. (1) into an equation with noncentered shot noise. We introduce Eq. (2) into Eq. (1) and write

$$\dot{X}(t) = \tilde{f}(X) + \zeta(t) , \tag{11}$$

where $\zeta(t)$ is noncentered shot noise given by

$$\zeta(t) = \sum_i \gamma_i \delta(t - \tau_i)$$

and

$$\tilde{f}(x) = f(x) - a ,$$

with a the mean value of $\zeta(t)$. We can now apply the results of Masoliver simply by replacing $f(x)$ by $\tilde{f}(x)$.

A. Jumps sizes exponentially distributed

In the evaluation of the MFPT to z we distinguish two situations: (i) $x_0 < z$ and (ii) $x_0 > z$. We call (i) *forward* MFPT and (ii) *backward* MFPT.

1. Forward mean-first-passage time

In this case $x_0 < z$ and the expressions for the MFPT are found in Sec. V B of [8] (critical levels at distinct sides of the fixed point). The MFPT is [cf. Eqs. (5.32)–(5.34) of [8]]

$$T_z^F(x_0) = \frac{1}{\gamma}\int_z^{x_0} \frac{dx}{f(x)-a} e^{\Phi(x)/D} \int_{x_s}^{x} dx' e^{-\Phi(x')/D} + \frac{1}{\lambda}\left(1 + \frac{1}{\gamma}\int_{x_s}^{z} dx\, e^{-[\Phi(x)-\Phi(z)]/D}\right) , \tag{12}$$

where $D = a\gamma$ and $a = \lambda\gamma$ [cf. Eqs. (6) and (8)]. The *effective potential function* $\Phi(x)$ is defined by

$$\Phi(x) \equiv -\int^x dx' \frac{f(x')}{1 - f(x')/a} . \tag{13}$$

As a simple application we have the case of the linear drift $f(x) = -x$ with $\gamma = \lambda = 1$. We obtain from Eq. (12)

$$T_z^F(x_0) = \frac{1}{x_0+1}(e^{1+x_0}-1) + \ln\frac{1+x_0}{1+z} - \mathrm{Ei}(1+x_0) + \mathrm{Ei}(1+z)\ , \quad (14)$$

where $\mathrm{Ei}(x)$ is the exponential integral function. Notice that, although z is an absorbing boundary, we have $T_z(z) \neq 0$. Equation (14) is shown in Fig. 2 along with simulations.

2. *Backward mean-first-passage time*

Now $x_0 > z$ and this case corresponds to Sec. V A of [8], i.e., critical levels (z, z_1) at one side of the fixed point. Since we are only interested in the MFPT to one critical level, we make the limit $z_1 \to \infty$ in Eqs. (5.5)–(5.7) of [8] with the result

$$T_z^B(x_0) = \frac{1}{\gamma}\int_z^{x_0} \frac{dx}{f(x)-a} e^{\Phi(x)/D} \int_\infty^x dx' e^{-\Phi(x')/D}\ . \quad (15)$$

For the linear case discussed above the result reads

$$T_z^B(x_0) = \ln\frac{1+x_0}{1+z} - \frac{1}{1+x_0} + \frac{1}{1+z} \quad (16)$$

(see Fig. 3). The difference between the MFPT's (12) and (15) comes from the consideration that the mechanism of level crossing is not equivalent in the forward and backward cases. In the forward case jumps only are responsible for the crossing because the ballistic motion between them takes the system away from z, while in the backward case it is *only* the ballistic motion that is responsible for the crossing, and jumps are not favorable events for a crossing to occur.

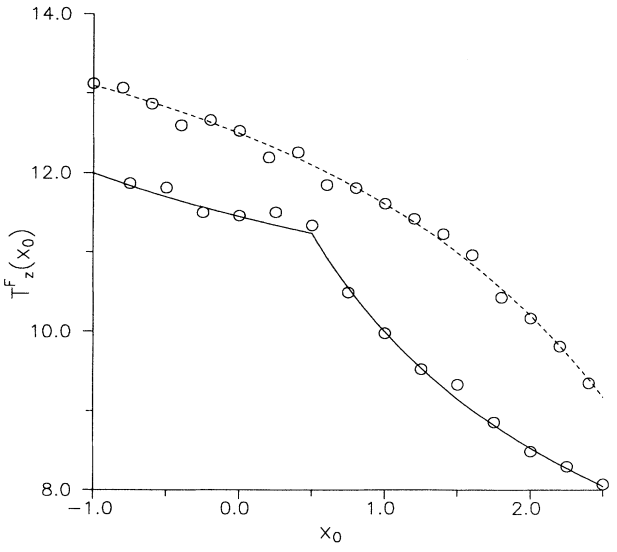

FIG. 2. Exact MFPT for white shot noise with linear drift $f(x) = -x$ ($a = 1$, $D = 1$, and $z = 2.5$). Exponential case (dashed line), Eq. (14), and jumps of the same size (solid line), Eq. (20). Circles represent simulation data (the standard deviation of the data is $\sigma = 0.2$).

B. Jumps of the same size

This case is surprisingly much more complicated than the one with exponentially distributed jumps. Masoliver [8] found that MFPT satisfies a differential equation with deviating arguments, with an initial function and a boundary condition. When $\gamma < z - x_s$ and for the *forward* case ($x_0 < z$) the equation reads

$$\frac{d}{dx_0}T(x_0) + \frac{\lambda}{f(x_0)-a}\left[T(x_0+\gamma) - T(x_0)\right] = -\frac{1}{f(x_0)-a}, \quad x_s < x_0 < z-\gamma\ . \quad (17)$$

This differential equation with delay is to be solved with the boundary condition

$$T(x_s) = T(x_s+\gamma) + \frac{1}{\lambda} \quad (18)$$

and the initial function

$$T(x_0) = \frac{1}{\lambda}\left(1 + Ce^{\lambda\rho(x_0)}\right), \quad z-\gamma < x_0 < z \quad (19)$$

where

$$\rho(x_0) = \int^{x_0} \frac{dx}{f(x)-a}.$$

The conditions given by Eqs. (18)–(19) are sufficient to determine a unique solution to the problem by the method of steps [13]. As an example we consider the solution to the linear case [$f(x) = -x$] when $a = 1$ and $D = 1$, which implies $\gamma = 2$ [cf. Eq. (9)]. In this case by the method of steps the solution is found to be

$$T(x_0) = \begin{cases} 2\left(1 + \frac{C}{\sqrt{1+x}}\right), & z-2 < x_0 < z \\ 4 + \frac{C}{\sqrt{1+x}}\left\{\ln\left[\sqrt{(x+1)(x+3)}\right] + x + 2\right\}, & -1 < x_0 < z-2 \end{cases} \quad (20)$$

where

$$C = \frac{2\sqrt{z-1}}{2 - \ln\left(\sqrt{z^2-1}+z\right)}. \quad (21)$$

We note that Eq. (20) is only valid in the range $1 < z < 3$.

This result is also plotted in Fig. 2 together with the result given by Eq. (14). We also observe that MFPT (20) has a discontinuity in the first derivative at $x = z - \gamma$. This is a common feature of differential equations with deviating arguments. In fact, at the end of the first step, the first derivative is continuous while the second derivative is discontinuous [13].

Unfortunately the method of steps becomes very complicated when there are more than two steps involved. The reason for this difficulty appears in the determination of the constant C [cf. (19)]. Since the value of C is obtained from the boundary condition (18) after *all the steps* have been carried out and the critical value x_s is reached. The same problem makes difficult the obtention of numerical solutions or even perturbative aproximations when γ is small.

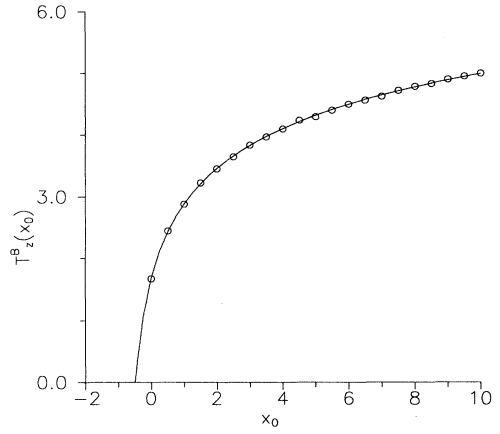

FIG. 3. Backward MFPT for WSN with exponentially distibuted jumps with linear drift $f(x) = -x$ ($a = 1$, $D = 1$, and $z = -0.5$), Eq. (16). Simulation data are represented by circles ($\sigma = 0.02$).

III. TRANSITON RATES FOR EXPONENTIALLY DISTRIBUTED JUMPS

As we have mentioned in Sec. I, when D is small and $a > a_c$ the system stays for a long time in the regions A or B and the transitions between these regions are suddenly occurring during times very short compared with the residence times in the regions A or B. In such a case the relationship between the MFPT and the transition rate from one well to the other of the bistable potential is [2]

$$r \sim \frac{1}{T_{\rm bot}} , \tag{22}$$

where $T_{\rm bot} = T_z(x_0)$ with $z = x_2$ and $x_0 = x_1$ (forward case) or $z = x_1$ and $x_0 = x_2$ (backward case).

The statement that D is small needs further clarification; it means that D must be small compared with the height of the effective potential barrier, i.e., $D << \Delta$ where $\Delta \equiv \Phi(x_u) - \Phi(x_0)$.

A. Forward transition rate

In this case $z = x_2$, $x_0 = x_1$, and Eq. (12) reads

$$T^F_{\rm bot} = \frac{1}{\gamma}\int_{x_2}^{x_1} \frac{dx}{f(x)-a} e^{\Phi(x)/D} \int_{x_s}^{x} dx' e^{-\Phi(x')/D} + \frac{1}{\lambda}\left(1 + \frac{1}{\gamma}\int_{x_s}^{x_2} dx\, e^{-[\Phi(x)-\Phi(z)]/D}\right). \tag{23}$$

If we assume that D is much smaller than the height of the effective potential barrier, then the integrand in the double integral in Eq. (23)—as a function of x—achieves its maximum in the neighborhood of $x = x_u$ [note that x_u is also the maximum of the effective potential $\Phi(x)$]. Hence the double integral in Eq. (23) can be split into the product of two single integrals which can be evaluated using Laplace's method [3]. Moreover, when D is small, the single integral in Eq. (23) is exponentially small. Taking all of this into account we finally get the asymptotic approximation

$$T^F_{\rm bot} \simeq \frac{2\pi}{(\alpha_1|\alpha_u|)^{1/2}} \left[1 + A_f D + O(D^2)\right] e^{\Delta^F/D} , \tag{24}$$

where Δ^F is the height of the effective potential barrier defined by

$$\Delta^F \equiv \Phi(x_u) - \Phi(x_1)$$

and

$$A_f \equiv \frac{\alpha_1}{12a^2} + \frac{\beta_1}{12a\alpha_1} - \frac{\alpha_u}{12a^2} - \frac{\beta_u}{12a\alpha_u} + \frac{5\beta_1^2}{24\alpha_1^3} - \frac{5\beta_u^2}{24\alpha_u^3} - \frac{3\delta_1}{4\alpha_1^2} + \frac{3\delta_u}{4\alpha_u^2} , \tag{25}$$

where

$$\alpha_{1,u} \equiv -f'(x_{1,u}),$$
$$\beta_{1,u} \equiv f''(x_{1,u}), \tag{26}$$
$$\delta_{1,u} \equiv -\frac{1}{6} f'''(x_{1,u}).$$

The forward transition rate is

$$r^F \sim \frac{(\alpha_1|\alpha_u|)^{1/2}}{2\pi} \left[1 - A_f D + O(D^2)\right] e^{-\Delta^F/D} . \tag{27}$$

The zeroth-order approximation of this rate is

$$r^F \sim \frac{(\alpha_1|\alpha_u|)^{1/2}}{2\pi} e^{-\Delta^F/D} , \tag{28}$$

in agreement with previous results [9].

A case of particular interest is that of a symmetric potential. In this case $f(x) = -x^3 + x$ and Eq. (24) reduces to

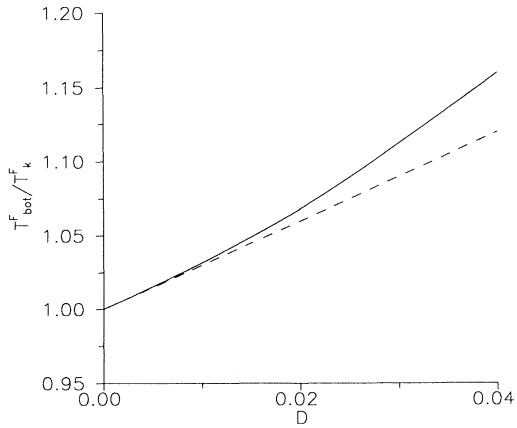

FIG. 4. Ratio of $T^F_{\rm bot}/T^F_k$ for the symmetric potential, $V(x) = x^4/4 - x^2/2$, and exponential WSN with $a = 0.5$. Exact result (solid line) obtained by numerical integration of Eq. (23) and asymptotic expansion (dashed line) as given as Eq. (29).

$$T^F_{\rm bot} \simeq \sqrt{2}\pi \left[1 + \left(\frac{3}{2} + \frac{1}{4a} + \frac{1}{4a^2}\right) D + O(D^2)\right] e^{\Delta^F/D} . \tag{29}$$

We note that in the Gaussian white-noise limit

$$a \to \infty,\ \lambda \to \infty,\ D = a^2/\lambda \text{ finite.}$$

Equation (29) yields the known first-order correction to the Kramers result [14]. We also note that the term

$$\left(\frac{1}{4a} + \frac{1}{4a^2}\right) D = \left(1 + \frac{1}{a}\right) \frac{\gamma}{4} \tag{30}$$

appears because of the non-Gaussian nature ($\gamma \neq 0$) of the WSN.

In Fig. 4 we plot the approximate MFPT (29) compared with the exact result obtained by numerical integration of Eq. (23). The figure shows the quotient $T^F_{\rm bot}/T^F_k$, where T^F_k is the zeroth-order approximation (i.e., the Kramers time) and is given by

$$T^F_k \equiv \frac{2\pi}{(\alpha_1|\alpha_u|)^{1/2}} e^{\Delta^F/D} .$$

We observe that when $\frac{\Delta^F}{D} \approx 10$ the agreement between the exact result and the approximation is within 5% of accuracy. Finally in Fig. 5 we show the exact result, the approximation (29), and numerical simulations.

B. Backward transition rate

In this case $z = x_1$, $x_0 = x_2$, and Eq. (15) reads

$$T^B_{\rm bot} = \frac{1}{\gamma} \int_{x_1}^{x_2} \frac{dx}{f(x) - a} e^{\Phi(x)/D} \int_{\infty}^{x} dx' e^{-\Phi(x')/D} . \tag{31}$$

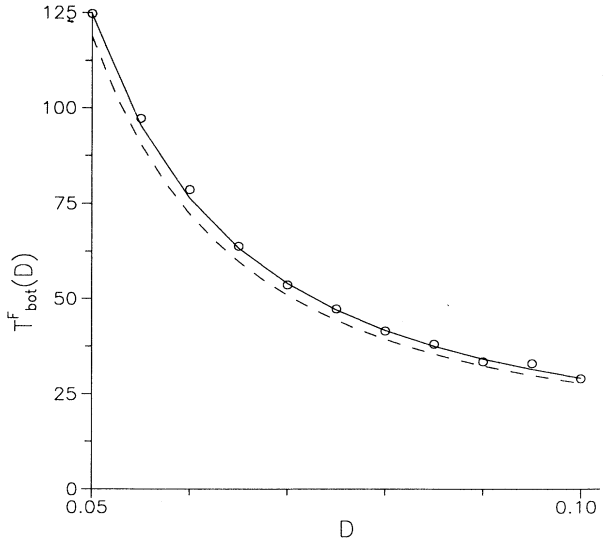

FIG. 5. Simulation data (circles) of $T^F_{\rm bot}$ in the exponential case for different values of D and $a = 0.5$ ($\sigma = 1.5$). Numerical integration of Eq. (23) (solid line) and asymptotic expansion, Eq. (29) (dashed line).

In the case of D small we follow the procedure outlined above to obtain

$$T^B_{\rm bot} \simeq \frac{2\pi}{(\alpha_2|\alpha_u|)^{1/2}} \left[1 + A_b D + O(D^2)\right] e^{\Delta^B/D} , \tag{32}$$

where Δ^B is the height of the effective potential barrier defined by

$$\Delta^B \equiv \Phi(x_u) - \Phi(x_2)$$

and

$$A_b \equiv \frac{\alpha_2}{12a^2} + \frac{\beta_2}{12a\alpha_2} - \frac{\alpha_u}{12a^2} - \frac{\beta_u}{12a\alpha_u} + \frac{5\beta_2^2}{24\alpha_2^3} - \frac{5\beta_u^2}{24\alpha_u^3} - \frac{3\delta_2}{4\alpha_2^2} + \frac{3\delta_u}{4\alpha_u^2} , \tag{33}$$

where α_2, β_2, and δ_2 are defined as in Eq. (26) by just replacing x_1 by x_2.

The backward transition rate is

$$r^B \sim \frac{(\alpha_2|\alpha_u|)^{1/2}}{2\pi} \left[1 - A_b D + O(D^2)\right] e^{-\Delta^B/D} . \tag{34}$$

As has been previously noticed [9] $\Delta^B > \Delta^F$, which implies $r^B < r^F$. This is a consequence of the asymmetry of the noise. Thus the δ peaks in the positive direction make that the MFPT be shorter in the forward case than in the backward case.

For a symmetric potential corresponding to $f(x) = -x^3 + x$ we have

$$T^B_{\rm bot} \simeq \sqrt{2}\pi \left[1 + \left(\frac{3}{2} - \frac{1}{4a} + \frac{1}{4a^2}\right) D + O(D^2)\right] e^{\Delta^B/D} . \tag{35}$$

This is shown in Fig. 6 along with the numerical inte-

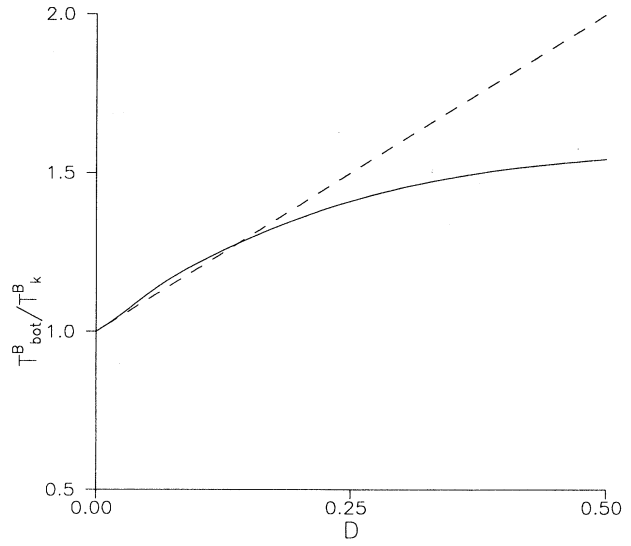

FIG. 6. Same as Fig. 4 but for the backward case, Eq. (35), and with $T^B_k = \sqrt{2}\pi e^{\Delta^B/D}$.

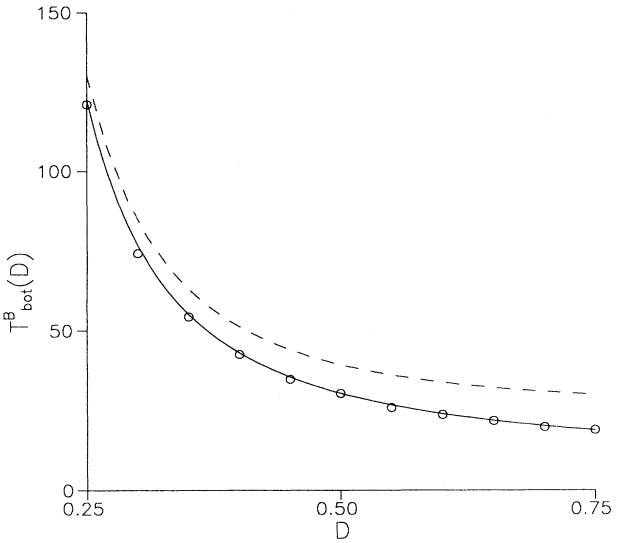

FIG. 7. Same as Fig. 5 but for the backward case.

gration of the exact result (31). We also show in Fig. 7 the agreement of the aproximate result with numerical simulations.

IV. MEAN-FIRST-PASSAGE TIME TO THE TOP OF THE BARRIER

Another case that has been extensively discussed in the literature is that of the MFPT from one of the minima to the maximum of the potential [15]. This quantity has been denoted by $T_{\rm top}$ to indicate passage to the "top of the barrier," although we should note that in the presence of noise, x_u is no longer the maximum of any "instantaneous potential" experienced by the system. This fact makes the physical interpretation of $T_{\rm top}$ less clear than that of $T_{\rm bot}$ and has elicited some discussion in the literature concerning the merits of calculating $T_{\rm top}$ when the driving noise is not Gaussian white. In spite of this consideration the calculation of $T_{\rm top}$ is still interesting. Thus for Gaussian colored noise there has been some controversy about the order of the corrections of this quantity. With the method presented above we can calculate exactly the order of these corrections for shot noise.

A. Forward case

We define $T^F_{\rm top} \equiv T^F_{x_u}(x_1)$. Then substituting $x_0 = x_1$ and $z = x_u$ into Eq. (12), assuming the weak-noise approximation and performing the integrals by Laplace's method, we finally obtain (up to second-order approximation in $D^{1/2}$)

$$T^F_{\rm top} \simeq \frac{\pi}{(\alpha_1|\alpha_u|)^{1/2}} \times \left[1 + B_f D^{1/2} + A_f D + O(D^{3/2})\right] e^{\Delta^F/D}, \tag{36}$$

where

$$B_f \equiv \frac{1}{3}\left(\frac{2}{\pi}\right)^{1/2}\left(\frac{\beta_u}{|\alpha_u|^{3/2}} + \frac{2|\alpha_u|^{1/2}}{a}\right) \tag{37}$$

and A_f is given by Eq. (25). For a symmetric potential we have

$$T^F_{\rm top} \simeq \frac{\pi}{\sqrt{2}}\left[1 + \frac{2}{3a}\left(\frac{2}{\pi}\right)^{1/2} D^{1/2} + \left(\frac{3}{2} + \frac{1}{4a} + \frac{1}{4a^2}\right) D + O(D^{3/2})\right] e^{\Delta^F/D}. \tag{38}$$

Another approximation of interest is the so-called "strong noise approximation," $D \gg 1$ and a finite. In this case the time interval between jumps and the noise intensity both grow at the same rate. In this limit we easily obtain from Eq. (12) the result

$$T^F_{\rm top} \sim \frac{1}{\lambda} + \frac{x_u - x_s}{a} + O\left(\frac{1}{D}\right). \tag{39}$$

We show in Fig. 8 the results given by Eqs. (38) and (39) along with the numerical integration of the exact result (12).

B. Backward case

Now $x_0 = x_2$. In the weak-noise approximation the asymptotic evaluation of the integrals appearing in Eq. (15) yields the result

$$T^B_{\rm top} \simeq \frac{\pi}{(\alpha_2|\alpha_u|)^{1/2}} \times \left[1 + B_b D^{1/2} + A_b D + O(D^{3/2})\right] e^{\Delta^B/D}, \tag{40}$$

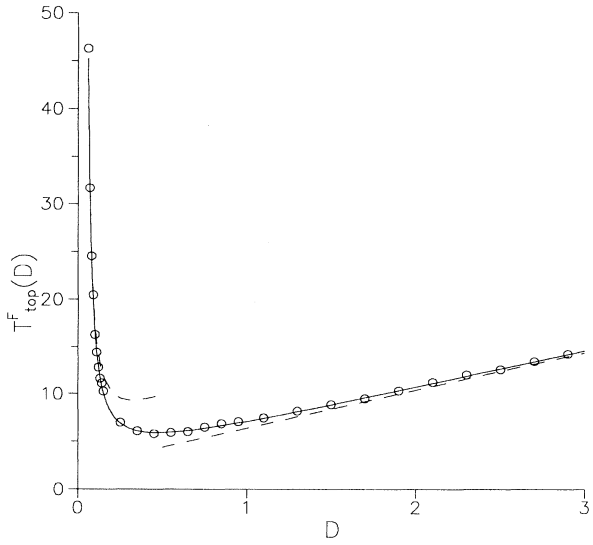

FIG. 8. $T^F_{\rm top}$ as a function of D for $a = 0.5$ and the symmetric potential. Exact result calculated numerically (solid line), simulation data (circles) and both aproximations Eq. (38), small D, and Eq. (39), intense noise (dashed line).

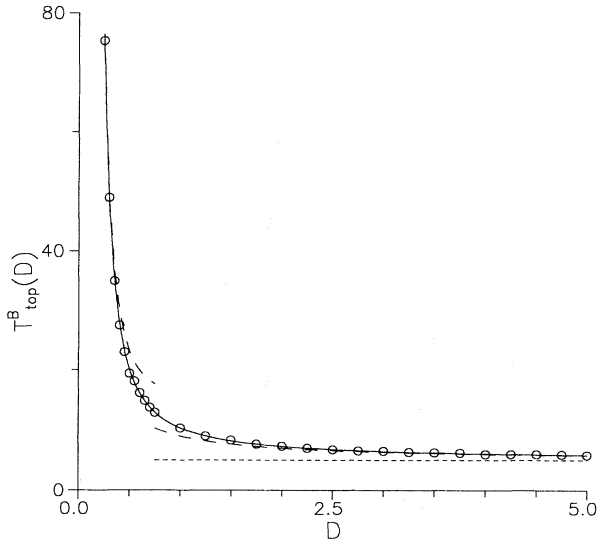

FIG. 9. Same as in Fig. 8 but for the backward case, Eqs. (42) and (43). The horizontal dashed line shows τ_{bal}.

where

$$B_b \equiv \frac{1}{3}\left(\frac{2}{\pi}\right)^{1/2}\left(-\frac{\beta_u}{|\alpha_u|^{3/2}}+\frac{|\alpha_u|^{1/2}}{a}\right) \tag{41}$$

and A_b is given by Eq. (33). For a symmetric potential we have

$$T^B_{top} \simeq \frac{\pi}{\sqrt{2}}\left[1+\frac{1}{3a}\left(\frac{2}{\pi}\right)^{1/2}D^{1/2}+\left(\frac{3}{2}-\frac{1}{4a}+\frac{1}{4a^2}\right)D +O(D^{3/2})\right]e^{\Delta^B/D}. \tag{42}$$

In this case the strong-noise approximation of Eq. (15) reads

$$T^B_{top} \sim \tau_{bal}+\frac{a^2}{2D}\left[\left(\int_\infty^{x_u}\frac{dx}{f(x)-a}\right)^2 -\left(\int_\infty^{x_2}\frac{dx}{f(x)-a}\right)^2\right]+O\left(\frac{1}{D^2}\right), \tag{43}$$

where

$$\tau_{bal}=\int_{x_2}^{x_u}\frac{dx}{f(x)-a}$$

is the ballistic time to reach the top of the barrier(see Fig. 9).

We finally note that either in the forward and backward case we have the ratio

$$\frac{T_{top}}{T_{bot}}=\frac{1}{2}+O(D^{1/2}). \tag{44}$$

This kind of behavior when D is small has been also observed for other input noises [3].

V. FORWARD MFPT FOR SHOT NOISE WITH JUMPS OF THE SAME SIZE

We are now interested in finding transition rates from one well to the other of a bistable potential when the system is driven by white shot noise with jumps of the same size. As we have noticed in Sec. II B, it is difficult to find closed expressions for the MFPT for this kind of shot noise. Moreover, one is not able to clearly define in which region of the parameter space (a,D) the transition rates exist because it is not even known which is the stationary probability density function for this process [7]. We have tried, however, to find approximations when γ is small (where the transition rate is assumed to exist). Nevertheless, either the approximation leads, when $a \to \infty$, to the transition rate of Gaussian white noise or it does not behave in a correct way. We should also mention that perturbative solutions to general differential equations with delay does not seem to be a well set topic in mathematics [13].

The idea of the perturbative scheme is to develop $T(x_0+\gamma)$ in powers of γ. In this way we find

$$T(x_0+\gamma)-T(x_0)=T'(x_0)\gamma+\frac{1}{2}T''(x_0)\gamma^2+O(\gamma^3). \tag{45}$$

If we now substitute Eq. (45) into Eq. (17) we obtain (to the lower power in γ) the equation

$$DT''(x_0)+f(x_0)T(x_0)=-1 \tag{46}$$

where D is given by Eq. (9). Equation (46) is the differential equation satisfied by the MFPT for a system like (1) with $F(t)$ being Gaussian white noise.

When γ is small the expansion of the boundary condition (18) reads

$$T'(x_s)=-\frac{1}{a}. \tag{47}$$

Now in the Gaussian white-noise limit

$$a \to \infty,\ \gamma \to 0,\ D=\frac{a\gamma}{2}\ \text{finite},$$

we see from Eq. (10) that $x_s \to -\infty$ and Eq. (47) yields

$$T'(-\infty)=0. \tag{48}$$

On the other hand, it is easily seen from Eq. (19) that the initial function satisfies the first-order differential equation

$$T'(x_0)-\frac{\lambda}{f(x_0)-a}T(x_0)=-\frac{1}{f(x_0)-a},$$

where $z-\gamma<x_0<z$. If we now develop this equation to lower orders in γ we get

$$T'(x_0)=\left(\frac{\gamma}{2D}-\frac{1}{\gamma}T(x_0)\right)[1+O(\gamma)] \tag{49}$$

$(z-\gamma<x_0<z)$. In the Gaussian white-noise limit we have $x_0 \to z$ and Eq. (49) yields

$$T(z)=0, \tag{50}$$

since $T'(x_0)$ is always finite. Equation (46) with bound-

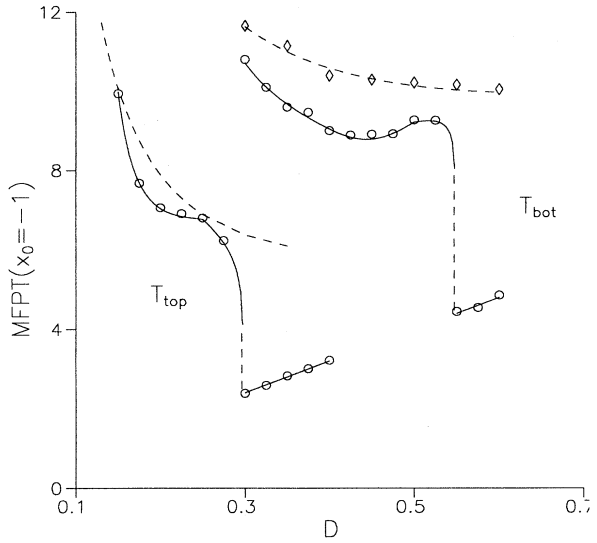

FIG. 10. $T_{\rm bot}$ and $T_{\rm top}$ for WSN with jumps of the same size when $a = 0.5$ (solid line). The same results for WSN with exponentially distributed jumps (for the same values of a and D) are shown in dashed line. Circles represent simulation data ($\sigma = 0.1$).

ary conditions (48) and (50) is the well-known problem of the MFPT to one critical level for white Gaussian noise [16].

Unfortunately, when this perturbative scheme is performed without allowing $a \to \infty$, we have not been able to obtain the correct aproximate boundary condition at z. In order to show how difficult it is to find an approximation, we have plotted in Fig. 10 the exact solution for $T_{\rm bot}$ and $T_{\rm top}$ (both numerically calculated) when no more than two steps are needed to reach the limit value. The example is for the symmetric case $f(x) = -x^3 + x$. In this case, the limit values of γ are

$$\gamma \geq |1 - x_s|/2$$

for $T_{\rm bot}$ and

$$\gamma \geq |x_s|/2$$

for $T_{\rm top}$. From the results of Fig. 10 we observe the following (we concentrate on $T_{\rm bot}$, although the same can be stated for $T_{\rm top}$)

(i) $T_{\rm bot}$ is discontinuous at $D = a|1-x_s|/2$. The reason for this discontinuity is that for greater values of D, γ is larger than the distance from x_s to z. Consequently, the system crosses with probability 1 in the first shot and $T_{\rm bot}$ is $1/\lambda$.

(ii) The first derivative of $T_{\rm bot}$ is discontinuous at $D = a$. The reason for this discontinuity is that if $D < a$, then $T_{\rm bot}$ is given by the expression of the MFPT after one step, but if $D > a$, then $T_{\rm bot}$ is given by the initial function (19). Both expressions have the same value at $D = a$, but the first derivative is discontinuous at this point.

These observations clearly show how difficult it is to obtain correct approximations for the case of jumps of the same size. This is to be contrasted with the much smoother behavior of the exponential case (also plotted in Fig. 10).

VI. CONCLUSIONS

We have obtained the expressions for the MFPT to one critical level for systems driven by centered WSN by using previous results for noncentered WSN [8].

For WSN with exponentially distributed jump sizes, we have obtained closed expressions for both the forward and the backward MFPT. For a general bistable system we have been able to get up to first order in D the transition rates, related with $T_{\rm bot}$ and compare them with previous results for WSN [9] and for Gaussian white noise [14]. Two asymptotic forms have been found for $T_{\rm top}$: the usual weak-noise aproximation and the intense noise approach (in this case the intensity of shots grows at the same rate as the interval between them). The different behavior of $T_{\rm top}$ when D increases is clearly explained by the asymmetry of the shot noise considered.

For WSN with jumps of the same size, we know the differential equation and the exact boundary conditions for MFPT. In this case we recover the well-known result for Gaussian white noise when $a \to \infty$ and $\gamma \to 0$ with $D = a\gamma/2$ finite. Nevertheless, we have not succeeded in finding, to lower orders in γ, any correction to the Gaussian white-noise result for the transition rate. The usual asymptotic methods are very difficult to apply because of the deviating argument in Eq. (17). Since we know the exact result we have also calculated numerically the solution for a particular case just to show the difficulties that arise out of the nonsmooth behavior of the MFPT when jumps are of the same size.

APPENDIX: PHASE DIAGRAM FOR BISTABLE SYSTEMS DRIVEN BY EXPONENTIALLY DISTRIBUTED SHOT NOISE

The stationary probability density $p_{\rm st}(x)$ for the random process (1) when $F(t)$ is white shot noise with an exponential distribution of jumps is given by [7]

$$p_{\rm st}(x) \propto \frac{1}{a - f(x)} e^{\Phi(x)/D}, \qquad x_s \leq x < \infty, \tag{A1}$$

where x_s is defined in Eq. (10) and $\Phi(x)$ is the effective potential (13). The interval $[x_s, \infty)$ is the region where $p_{\rm st}(x)$ is defined positive and it depends on the values of parameter $a = \lambda\gamma$.

Let a_c be the value of $f(x)$ at its local maximum. If $a < a_c$ the equation $f(x) - a = 0$ has three real roots (x_1', x_2', x_u'). In this case the action of the noise consists in making the system jump to the right of x_2', but once the system is in that region stays there forever. Therefore, if $a < a_c$ the noise only induces transitions in the forward direction and bistability is broken. On the other hand, if $a > a_c$, then $f(x) - a = 0$ has only one real root $x_s < x_1$ and transitions take place in both directions.

The equation that gives the extremes of $p_{\rm st}(x)$ is

$$f(x) + \frac{D}{a} f'(x) = 0 \tag{A2}$$

and depending on the values of D and a the stationary probability density function will have maxima or minima in its domain. Moreover, we can also study in great detail the behavior of $p_{\rm st}(x)$ near x_s. With all of these elements: the domain, the extremes, and the behavior near x_s we can obtain a qualitative portrait of the stationary probability density function. This portrait, which depends on the parameters D and a, is called *phase diagram* and allows us to know which are the bistability regions of the system.

For a symmetric potential $f(x) = -x^3 + x$, Eq. (A1) reads

$$p_{\rm st}(x) \propto \Theta(x - x_s) \frac{(x - x_s)^{\alpha - 1}}{(x^2 + x x_s + x_s^2 - 1)^{1+\alpha/2}} \times \exp\left[-\left(\frac{x}{\gamma} + \alpha g(x) \right) \right] , \tag{A3}$$

where $\Theta(x)$ is the Heaviside step function $\alpha \equiv \frac{a^2/D}{3x_s^2 - 1}$ and

$$g(x) = \frac{3x_s}{\sqrt{3x_s^2 - 4}} \arctan\left(\frac{2x + x_s}{\sqrt{3x_s^2 - 4}} \right) .$$

In this case $a_c = 2/3\sqrt{3}$ and the behavior of $p_{\rm st}(x)$ near x_s is determined by the term $(x - x_s)^{\alpha - 1}$. Thus, if $\alpha < 1$, then the stationary density diverges in the neighborhood of x_s. If $1 < \alpha < 2$, $p_{\rm st}(x)$ does not diverge, but its first derivative does. When $\alpha > 2$ both the density and its derivative are zero at $x = x_s$. Finally, the position of the extremes is given by the roots of the equation $-x^3 - 3\gamma x^2 + x + \gamma = 0$. The phase diagram is shown in Fig. 11.

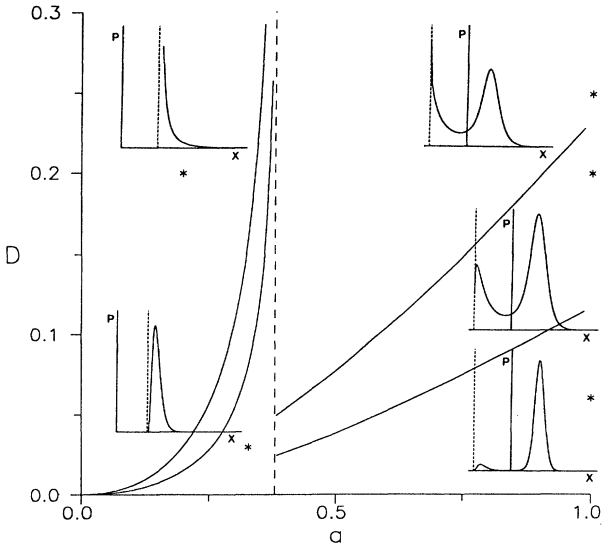

FIG. 11. Different forms of the stationary probability density (phase diagram) for the system described by Eq. (1) with $f(x) = -x^3 + x$ and $F(t)$ WSN with exponentially distributed jump sizes. The stars represent the parameter values (a, D) for which different stationary probability density functions are shown in the diagram.

We finally mention that there are no similar calculations for shot noise with jumps of the same size [7].

[1] *Noise in Nonlinear Dynamical Systems*, edited by F. Moss and P.V.E. McClintock (Cambridge University Press, Cambridge, England, 1989), Vols. 1–3.

[2] P. Hänggi, P. Talkner, and M. Borkovek, Rev. Mod. Phys. **62**, 251 (1990).

[3] J.M. Porrà, J. Masoliver, and K. Lindenberg, Phys. Rev. A **44**, 4866 (1991).

[4] J.M. Porrà, J. Masoliver, K. Lindenberg, I. L'Heureux, and R. Kapral, Phys. Rev. A **45**, 6092 (1992).

[5] N.G. Van Kampen, Physica **102A**, 489 (1980).

[6] V.I. Klyatskin, Radiophys. Quantum Electron. **20**, 382 (1977).

[7] C. Van den Broeck, J. Stat. Phys. **31**, 467 (1983).

[8] J. Masoliver, Phys. Rev. A **35**, 3918 (1987).

[9] C. Van den Broeck and P. Hänggi, Phys. Rev. A **30**, 2730 (1984).

[10] P. Hänggi and P. Talkner, Phys. Rev. A **32**, 1934 (1985).

[11] E. Hernández-Garcia, L. Pesquera, M.A. Rodriguez, and M. San Miguel, Phys. Rev. A **36**, 5774 (1987).

[12] J. Masoliver, K. Lindenberg, and B. J. West, Phys. Rev. A **34**, 2351 (1986); M.A. Rodriguez and L. Pesquera, *ibid.* **34**, 4532 (1986); V. Balakrishnan, C. Van den Broeck, and P. Hänggi, *ibid.* **38**, 4213 (1988); J. Masoliver, J.M. Porrà, and G.H. Weiss, *ibid.* **45**, 2222 (1992).

[13] L.E. El'sgol'ts and S.B. Norkin, *Introduction to the Theory and Applications of Differential Equations with Deviating Arguments* (Academic, New York, 1973).

[14] R.S. Larson and M.D. Kostin, J. Chem. Phys. **69**, 4821 (1978).

[15] K. Lindenberg, B.J. West, and J. Masoliver, in *Noise in Nonlinear Dynamical Systems*, edited by F. Moss and P.V.E. McClintock (Cambridge University Press, Cambridge, England, 1989), Vol. 1.

[16] C.W. Gardiner, *Handbook of Stochastic Methods* (Springer-Verlag, Berlin, 1983).